ACS Sustainable Chemistry & Engineering

Research Article

pubs.acs.org/journal/ascecg

# Poly Tri-s-triazines as Visible Light Sensitizers in Titania-Based Composite Photocatalysts: Promotion of Melon Development from Urea over Acid Titanates

Dangguo Gong,[†,‡] James George Highfield,*[,‡] See Zhong Edison Ng,[†] Yuxin Tang,[†] Weng Chye Jeffrey Ho,[†] Qiuling Tay,[†] and Zhong Chen*[,†]

[†]School of Materials Science and Engineering, Nanyang Technological University, 50 Nanyang Avenue, Singapore 639798, Singapore

[‡]Heterogeneous Catalysis Technology, Institute of Chemical & Engineering Sciences, 1 Pesek Road, Singapore 627833, Singapore

Supporting Information

**ABSTRACT:** Photocatalysis has become increasingly popular for applications in the energy and environmental fields. However, in its conventional form as a pristine (white) semiconductor oxide, e.g., titania ($TiO_2$), the photocatalyst has a wide band gap and does not respond to a large fraction of the solar power available across the visible region. Recently, some success has been reported in the in situ synthesis and deposition of melon [poly (tri-s-triazine) with an empirical formulation of $H_3C_6N_9$] onto $TiO_2$ to act as a visible sensitizer. In the present contribution, we report the interesting finding that composites based on hydrogen titanate cores bearing shells of melon and the related graphitic carbon nitride (g-$C_3N_4$) as sensitizers are far superior in simulated solar (visible) light-driven photodegradation of methyl orange (MO) dye and ethanol photo-oxidation as compared to the individual components. These layered titanate nanotubes/nanobelts also offer a practical advantage by promoting the build-up of melon from urea as compared to anatase $TiO_2$. This is believed to be linked to the higher density coverage of titanates by surface OH groups and their Brønsted acidic properties, which promote polymerization. Development of the melon structure was verified by diffuse reflectance infrared spectroscopy (DRIFTS) and solid-state nuclear magnetic resonance ($^{13}C$ NMR). The melon layer was found to be fully developed after thermal activation at ~400 °C and photostable under open beam irradiation. More severe heat treatment led to melon degradation, as confirmed by TGA, and loss of visible-responsive photocatalytic activity.

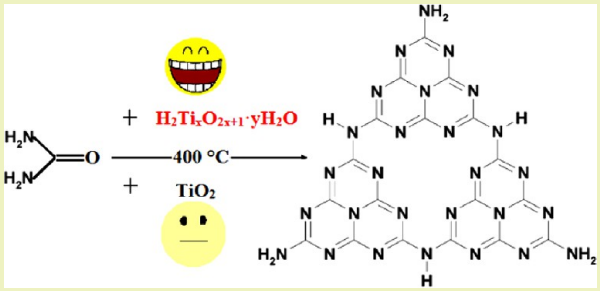


**KEYWORDS:** *Photocatalysis, Hydrogen titanates, Melon, Graphitic carbon nitride, Visible light sensitization*

## INTRODUCTION

Since the discovery of photo-assisted water splitting over a $TiO_2$ surface in 1972,[1] photocatalysis has developed into the method of choice in driving a range of light-to-energy storage processes,[2−5] e.g., alcohols reforming, advanced oxidation processes for environmental remediation, self-cleaning surfaces, etc. While titania ($TiO_2$) is an excellent photocatalyst, it has one key limitation. Because of its wide band gap (3.2 ev for anatase $TiO_2$), it only responds to ultraviolet (UV) light, which constitutes less than 5% of the solar power spectrum. For better use of sunlight, ways of "sensitizing" $TiO_2$ to the visible range have been under intensive investigation in the past decade. Historically, the most popular approach has been by doping with color centers, such as transition metal cations, but with mixed results. This has been superseded by attempts to "narrow" the band gap of $TiO_2$ using anion dopants, most popularly N, C, and S.[6,7]

Although N-doped $TiO_2$ has been extensively studied, the origin of the visible light response is still under debate. Most of the preparation methods use an organic compound as the nitrogen source in a "wet" chemical process, usually followed by calcination at mild temperature. The choice of the N source, as well as the preparative conditions, has a large influence on the photocatalytic activity in the resulting product, possibly due to the presence of chemically diverse nitrogen species, such as oxidic (NO$x$), nitridic ($N^{3-}$), or amidic (NHy).[3,6] Because of their relative abundance and low price, the most commonly used nitrogen sources are urea and its derivatives. Careful recent studies by Mitoraj and Kisch[8−10] have clearly proved that a condensed polymeric layer of melon is formed from urea on the $TiO_2$ surface and that this is the chromophore responsible for visible light activity. As this surface-overlayer-based system is quite distinct from the (bulk) doped type, they state that it is best classified as "melon-modified" $TiO_2$. In the recent review by H. Kisch,[11] it was suggested that the visible light activities of the many samples previously reported as "C- or N-doped" in fact do not contain true lattice-doped atoms or related oxygen vacancies. Melon, one stable polymer built from

Received: May 31, 2013
Revised: September 2, 2013
Published: October 7, 2013

  

tri-s-triazine units, with an empirical formula of $H_3C_6N_9$, was given the name by Liebig more than 150 years ago.[12−14] The formation of melon from urea is a condensation process involving the surface hydroxyl groups of the substrate. It can be conveniently divided into three stages:[9,10] (1) thermal decomposition of urea into isocyanic acid and ammonia at 320−400 °C (eq 1) and (2) melamine formation by the reaction of iscocyanic acid (and/or cyanamide) with surface OH groups of $TiO_2$ (eqs 2 and 3). As shown in eq 4, the overall process is melamine formation from urea in the presence of $TiO_2$ at 400 °C. Finally (stage 3), melamine undergoes polycondensation to form melem, melam, and finally melon. The (yellow) melon is believed to be the principal structure conferring visible light sensitization.

$$(NH_2)_2CO \xrightarrow{320\sim400^{\circ}C} HNCO + NH_3 \quad (1)$$

$$\equiv Ti-OH + O=C=N-H \rightarrow \equiv Ti-NH_2 + CO_2 \quad (2)$$

$$\equiv Ti-NH_2 + H-O-C\equiv N \rightarrow \equiv Ti-OH + H_2N-C\equiv N \quad (3)$$

$$6(NH_2)_2CO \xrightarrow{400^{\circ}C/TiO_2} C_3H_6N_6 + 6NH_3 + 3CO_2 \quad (4)$$

The related fully condensed polymer is known as graphitic carbon nitride (g-$C_3N_4$). It is the final deamination product in the series of ammonocarbonic acids and shares the same tri-s-triazine units with melon. A narrow band gap semiconductor (Eg ∼2.7 eV) g-$C_3N_4$ is of growing interest as a photocatalyst[15,16] and has been extensively studied in water splitting[16−18] and in combination with $TiO_2$[19,20] for visible light-driven degradation of organic pollutants.

Nanostructured layered titanates are of great interest for catalytic purposes. Their large surface areas and ion-exchange properties provide the possibility to achieve uniform and high loading of the active noble metal in a highly dispersed form on the surface.[21−23] They also provide a good platform for delicate phase and morphological tailoring by annealing[24,25] or wet chemistry reaction.[26,27] However, introducing additional functional molecules on their surfaces by utilizing their chemical properties has seldom been explored.[28]

Recently, we reported the synthesis of a "N-doped" dual-phase titanate/$TiO_2$ composite by a one-pot solvothermal method that is able to degrade methylene blue (MB) under visible light irradiation.[29] In a subsequent study of phenol degradation,[30] visible activity was thought to derive from a chromophore linked to Ti−N surface bonds in a polyunsaturated hydrocarbonaceous overlayer, along with bulk doping by N.

In this contribution, we report that titanates/$TiO_2$ bearing poly (tri-s-triazine) overlayers, viz., melon and g-$C_3N_4$ as photostable sensitizers, show far superior catalytic activity than the isolated compounds in both photodegradation of methyl orange (MO) dye and photo-oxidation of ethanol vapor under visible light irradiation. In addition, titanate substrates promote the spontaneous build-up of the melon overlayer and the related growth in photoactivity as compared to anatase $TiO_2$. A tentative mechanism explaining the synergy in these composites for photo-oxidation catalysis is proposed.

## EXPERIMENTAL SECTION

**Materials Synthesis.** Titanates were synthesized through a conventional hydrothermal method.[21] The detailed procedure is as follows. Anatase $TiO_2$ (Aldrich, 99.8%) powder (2 g) was suspended in 10 M NaOH (Schedelco, grade A.R.) solution (50 mL), sonicated for 30 min, and then transferred to a Teflon autoclave. The slurry was then heated to 150 °C (for nanotubes) or 200 °C (for nanobelts) and held at this temperature for 48 h. The recovered samples were washed several times in deionized water until the pH was lowered to 9 and then washed in 0.1 M $HNO_3$ to ion-exchange any residual $Na^+$ ions for $H^+$ before oven drying at 80 °C. The sample is denoted as HT 150 or HT 200, indicating that it was synthesized at 150 or 200 °C and proton-exchanged.

To obtain melon-modified titanates, 500 mg of HT 150 and HT 200, along with commercial anatase $TiO_2$ controls, were dispersed in a urea solution (1 g of urea dissolved in 40 mL ethanol), and the mixtures were dried with continuous stirring at 70 °C. After ethanol was evaporated, the white powders were recovered and heat treated (ramp rate: 5 °C/min) in a quartz tube up to 400 °C and then held at 400 °C for 2 h in dry nitrogen flow.

Graphitic carbon nitride (g-$C_3N_4$) was prepared through thermal polymerization of dicyandiamide in air up to 550 °C for 4 h. Then, samples of g-$C_3N_4$ and titanate nanotubes (HT 150) mixed in different ratios were heated to 400 °C in dry nitrogen flow to yield g-$C_3N_4$ modified samples.

**Materials Characterization.** To identify the crystalline structure and phase transformation of the samples, X-ray diffraction (XRD) measurements were performed on a Shimadzu 6000 powder diffractometer equipped with a Cu K$\alpha$ source. The morphology and particle size of the samples were investigated by JEOL 2010 transmission electron microscopy (TEM), operating at an accelerating voltage of 200 KV. Brunauer−Emmett−Teller (BET) surface areas and pore diameters were determined by $N_2$ physisorption (at 77 K) on a Micromeritics ASAP 2420 surface area and porosity analyzer. All solid-state MAS $^{13}C$ NMR spectra were recorded with a Bruker Ultrashield AVANCE 400WB (400 MHz) spectrometer with a spin rate of 5000 $s^{-1}$. The weight percentages of C, N, and H of the surface species were analyzed by a Euro Vector EA 3000 series elemental analyzer. The optical absorption spectra of samples were measured on a Shimadzu 3600 UV−vis-NIR spectrometer in diffuse reflectance (DR) mode over the range of 200−800 nm against a $BaSO_4$ standard.

The thermal stability of the samples was investigated in a Setaram Setsys 12 thermo-balance. Diffuse reflectance infrared fourier transformed spectroscopy (DRIFTS) was employed to identify surface functional groups and surface reactions. It consisted of a heatable reaction cell (HVC-DRP, Harrick Scientific) mounted into a Praying Mantis (Harrick Scientific) optical accessory located in the front sample compartment of a Digilab Excalibur FTS-3000 FTIR spectrometer (Varian, Inc.). The reaction cell was fitted with a pair of $CaF_2$ windows for incident and remitted IR radiation and a quartz window for optical pumping from an Oriel 150W Xe DC short arc lamp. The UV−vis pump beam was directed onto the sample via a suitably clamped 1 m in length high-grade fused quartz light pipe with a focusing adapter. For visible light experiments, a filter cutting off wavelengths below 400 nm was inserted into the holder at the exit from the lamp housing. Gas flow was conveniently tapped off the mass-flow controlled supply from the Setaram thermobalance. The detailed configuration of the TG-DRIFTS setup is described in a previous publication.[2]

**Photocatalytic Testing.** Methyl orange (MO) was chosen as the target molecule to assess the photocatalytic performance of photocatalysts in liquid suspension. For each experiment, 50 mg of photocatalyst was dispersed into 50 mL of MO solution at a concentration of 10 ppm and stirred for 2 h in the dark before illumination to establish the adsorption/desorption equilibrium. An Asahi spectra HAL 320 high power xenon lamp was used as the light source, and the intensity was set to 120 mW $cm^{-2}$. A "super cold" filter was interposed to remove infrared radiation and minimize evaporative losses for the full spectrum UV−vis test. For visible light (VIS) experiments, an additional optical filter was used to remove radiation below 385 nm. The concentration change in MO was determined periodically on extracted aliquots based on its absorption peak at 464.5 nm using a Shimadzu UV−vis 2501 spectrometer.

For photo-oxidation of ethanol, the alcohol was vaporized in the TGA furnace and then delivered to the FTIR spectrometer by a

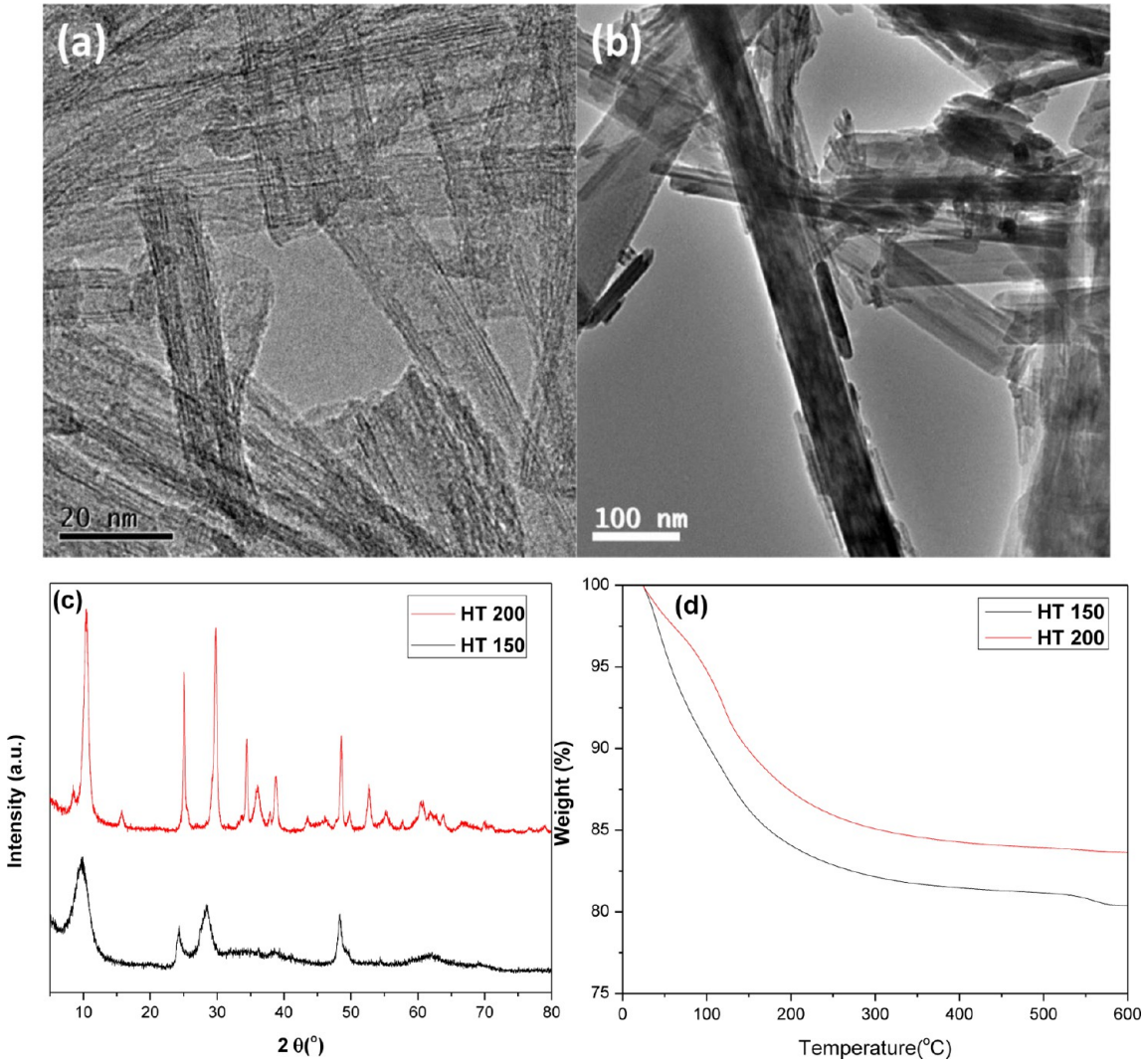


**Figure 1.** Characterization of titanates: TEM images of (a) HT 150 and (b) HT 200, (c) XRD patterns, and (d) TGA curve measured at 10 °C/min from RT to 600 °C in $N_2$ flow.

purified nitrogen carrier flow. The DRIFTS cell was then isolated for static tests before starting illumination. In situ time-resolved DRIFT spectra were collected and averaged every 2 min using the kinetics mode of the Resolutions Pro 4a software over the range of 4000−1000 $cm^{-1}$ at 4 $cm^{-1}$ resolution.

## RESULTS

**Characterization of Hydrogen Titanate.** Typical TEM images of the titanate are shown in Figure 1a and 1b. As-prepared titanate nanotubes (TNTs) had lengths up to hundreds of nanometers, outer diameters of around 10 nm, and inner diameters around 5 nm. Titanate belts (TNBs) had lengths from hundreds of nanometers to several micrometers, with widths from tens to hundreds of nanometers. Their layered structure could be identified from the peaks around 10° in the XRD pattern, and the interlayer distance was estimated to be around 0.96 nm (Figure 1c). Because of their tubular structure, TNTs had a large surface area, around 176 $m^2\ g^{-1}$, while the surface area of TNBs was only around 35 $m^2\ g^{-1}$.

**Formation of Melon from Urea on Titanate/$TiO_2$.** As shown in Figure 1d, pure titanates are thermally unstable, losing weight through dehydration before undergoing phase transformation above ~300 °C.[22−24] In the present work, urea was mixed with either titanate or commercial anatase $TiO_2$ in a weight ratio of 2:1 and then annealed in $N_2$ gas. Elemental analysis (EA) provided essential information about the deposited surface products, as shown in Table 1. By comparison, annealing in air resulted in lower loadings of C and N (Table S1, Supporting Information), suggesting some oxidation and evolution of gaseous products. The atom ratios of C to N were also calculated as shown in the far right column of Table 1. There are 18 carbon atoms and 27 nitrogen atoms in a single formula unit of melon, so the theoretical atom ratio of C to N is 0.667. The C/N ratios of the samples annealed under nitrogen were fairly close to the theoretical value. It is also interesting to note that more surface species were formed on HT 150 and HT 200 as compared to anatase $TiO_2$.

**Table 1. Elemental Analysis Results of Melon-Modified Titanate/$TiO_2$ Samples Calcined at 400 °C in $N_2$**

| samples ($N_2$) | H (wt %) | C (wt %) | N (wt %) | C/N (mole ratio) |
|---|---|---|---|---|
| urea−HT150 | 1.72 | 6.55 | 11.45 | 0.667 |
| urea−HT200 | 0.86 | 5.45 | 10.57 | 0.602 |
| urea−anatase | 0.12 | 1.56 | 2.32 | 0.784 |


dx.doi.org/10.1021/sc400162p | ACS Sustainable Chem. Eng. 2014, 2, 149−157

XRD patterns of the mixtures annealed in nitrogen flow up to 400 °C are shown in Figure 2. It is notable that HT150 did

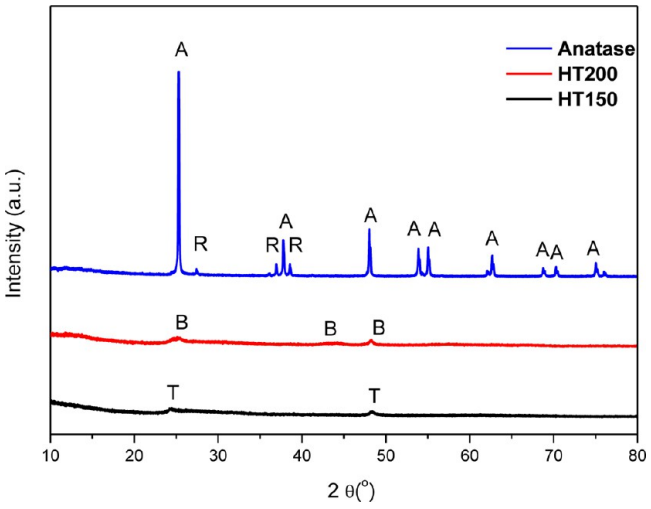


**Figure 2.** XRD patterns for mixed samples annealed in nitrogen flow at 400 °C. "A" denotes anatase phase $TiO_2$. "R" denotes rutile phase $TiO_2$. "B" denotes $TiO_2$(B) phase. "HT" denotes titanate phase $TiO_2$.

not fully transform into anatase phase. Rather, it partially retained the titanate structure, while HT 200 transformed to a monoclinic phase $TiO_2$(B). The morphologies of calcined samples are shown by TEM in Figure 3. HT 150 kept its tubular structure, and some scattered deposits of polymeric melon could be seen. The morphology of HT 200 and anatase $TiO_2$ did not change much, and little or no melon was evident.

The surface species after calcination in $N_2$ were also examined by $^{13}C$ solid-state nuclear magnetic resonance (NMR). As shown in Figure 4, three resonances were evident for HT 150 and HT 200 at ~165, 163, and 156 ppm, whereas there was only a weak singlet at ~165 ppm for the modified anatase sample. The low-field signals ($\delta$ = 163−165 ppm) and the high-field signal ($\delta$ = 157 ppm) could be assigned to $CN_2(NH_x)$ and $CN_3$ moieties in tri-s-triazine (heptazine), respectively,[31−33] confirming the formation of melon on the surfaces of HT 150 and HT 200.

Optical properties of the melon-modified samples were examined by diffuse reflectance (DR) UV−visible spectroscopy as shown in Figure 5. Melon-modified titanate samples HT 150 and HT 200 had more intense visible light absorption compared to melon−anatase, showing broad tails extending beyond 500 nm. This correlates with the higher loadings of melon as indicated by EA and NMR. Accordingly, the titanates

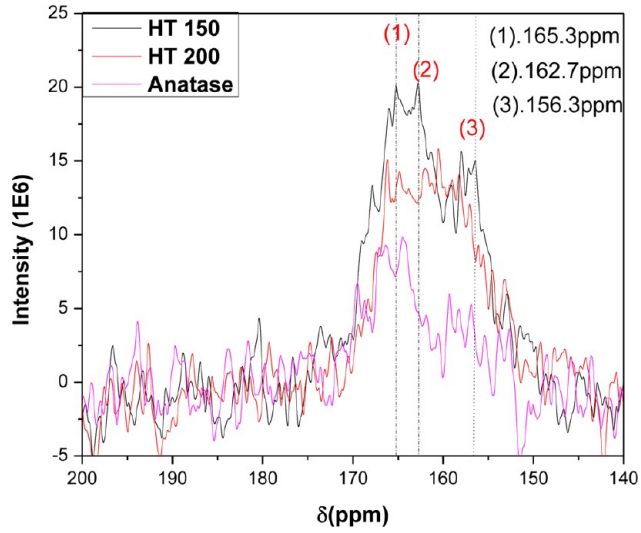


**Figure 4.** Solid-state $^{13}C$ NMR spectra of melon modified samples.

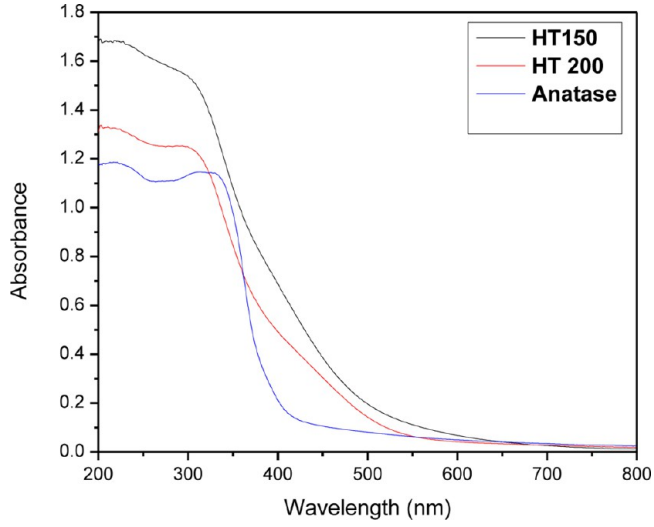


**Figure 5.** Diffuse reflectance UV−vis spectra of melon-modified samples calcined at 400 °C in $N_2$.

were yellow-brown in appearance, as compared to a pale yellow hue in anatase $TiO_2$.

Melon formed on the surface could be removed by thermal oxidation. TGA curves in Figure 6 show the weight changes of melon-modified samples during heating in air up to 800 °C. The furnace temperature was ramped and held at 100 °C for 40 min to remove physically adsorbed moisture for better

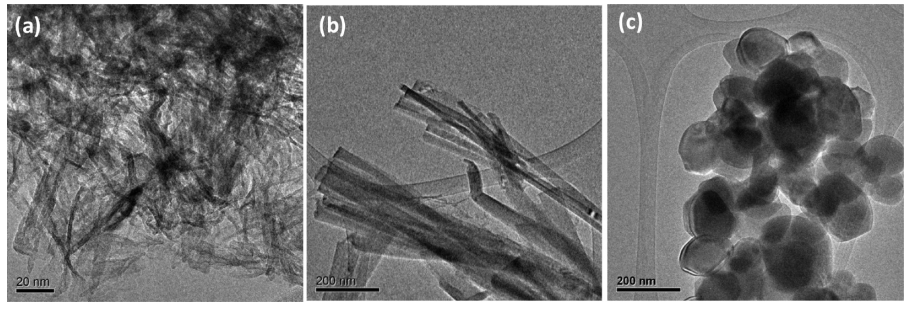


**Figure 3.** TEM micrographs of melon-modified samples calcinated at 400 °C in nitrogen gas: (a) HT 150, (b) HT 200, an d (c) anatase.


dx.doi.org/10.1021/sc400162p | ACS Sustainable Chem. Eng. 2014, 2, 149−157

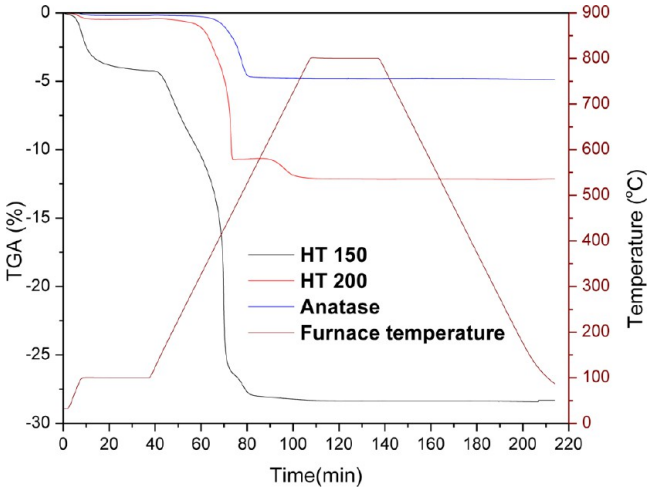


**Figure 6.** Relative weight changes of melon-modified samples when heating to 800 °C in air.

estimation of melon amount and reactivity. After predrying, the furnace was ramped to 800 °C at 10 °C/min. A sharp decrease in weight was observed in all cases just above 400 °C, corresponding to depolymerization, oxidation, and volatilization. This indicated that the ideal temperature for melon formation is around 400 °C. All samples reached a steady weight by 500 °C, suggesting complete removal of melon. The "dry" weight loss was 24% for melon−HT 150, 12% for melon−HT 200, and ∼5% for melon−anatase. These values corresponded quite well to the sum of weight percentages of hydrogen, carbon, and nitrogen from elemental analysis seen in Table 1. After this severe oxidation treatment, all previous visible absorption was removed (Figure S1, Supporting Information), confirming the residues were back in the virgin (oxide) state.

**Surface Species Identification and Photostability by DRIFTS.** Figure 7 compares the DRIFT spectra of modified samples against unsupported melon as the reference, whose peaks have been assigned elsewhere as follows:[12] 810 $cm^{-1}$, 6-membered ring out of plane bending; 1250 $cm^{-1}$ and 1324 $cm^{-1}$, $\nu(C-N)_{chain}$ between the heptazine ring and NH group; 1414 $cm^{-1}$, $\delta(NH)$; 1468 $cm^{-1}$, $\nu$(ring); 1640 $cm^{-1}$, $\delta(NH_2)$ conjugated with heptazine ring; and 3190 and 3300 $cm^{-1}$, $\nu(NH)_{sym/asym}$. The most distinct melon bands were also evident in the modified samples, viz., 1640, 1414, 1468, 3190, and 3300 $cm^{-1}$. The existence of these IR bands strongly supports the formation of melon on the surfaces, with intensities in proportion to the loading as determined by EA analyses.

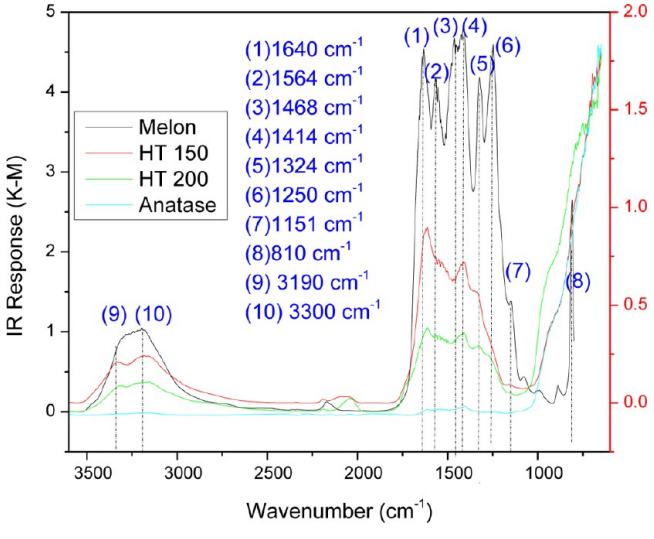


**Figure 7.** DRIFT spectra of melon and melon-modified samples. To improve spectral quality, samples were diluted to 5 wt % in KBr and spectra were collected after pre-drying at 200 °C in $N_2$.

For surface-sensitized photocatalysts, the stability of the sensitizer under applied conditions is essential. It is well known that organic dyes and pollutants like methylene blue and methyl orange are photodegraded under UV−vis light. Before using melon as an organic polymeric sensitizer, it was important to verify its photostability. Figure 8 shows DRIFT spectra of melon−HT 150 collected after various exposure times under UV−vis irradiation in air. For neat melon−HT 150, the intensity of IR response was very strong, but the characteristic bands of melon were still distinguishable. During photoirradiation up to 16 h, the bands remained virtually unaffected, indicating that melon is a photostable sensitizer.

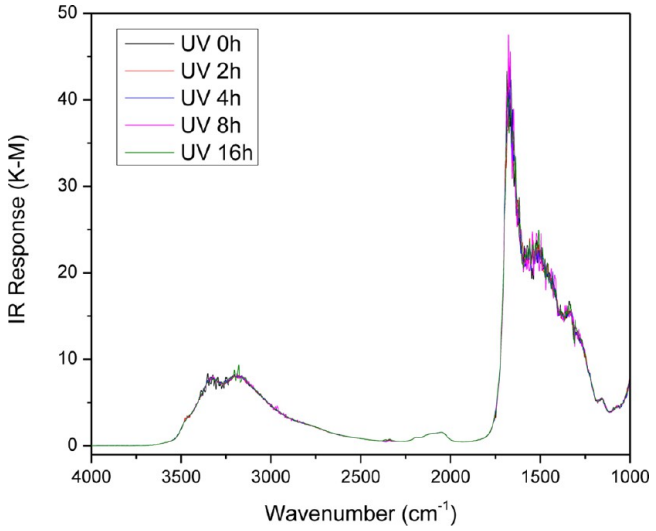


**Figure 8.** DRIFT spectra of melon-modified HT 150 under UV−vis irradiation in air for 16 h.

**Photocatalytic Reactor Tests of Melon-Modified Samples.** *Photodegradation of Methyl Orange under Visible Light Irradiation.* Methyl orange (MO) dye was selected as a model for the photocatalytic performance test, as it is a pollutant found in wastewater from the textile industry and is unaffected by direct photolysis.[23] Pristine titanate and anatase $TiO_2$ have been extensively studied. Adsorption of MO by titanate and $TiO_2$ in the dark is negligible, and neither shows significant photocatalytic activity under visible light (>385 nm).[23] Figure 9 shows the effect on MO of visible light irradiation in the presence of suspended particles of melon-modified samples. It was found that melon−HT 150 shows around 80% degradation within 4 h, while melon−HT 200 and melon−anatase exhibited about 30% and 10% degradation, respectively. Visible light photocatalytic activity is clearly conferred by the presence of melon. The higher activity of melon−HT 150 is probably due to its better light absorption in the visible light region and more efficient charge transfer between the surface melon layer and tubular titanate substrate


dx.doi.org/10.1021/sc400162p | ACS Sustainable Chem. Eng. 2014, 2, 149−157

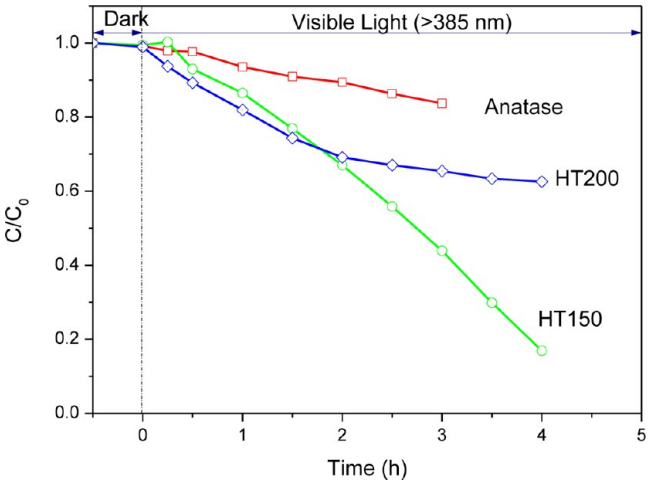


**Figure 9.** Photocatalytic degradation of MO solution (5 ppm) by melon-modified samples under visible light irradiation (>385 nm).

that allow efficient activation of oxygen and formation of reactive radicals.

*Photo-Oxidation of Ethanol under Visible Light Irradiation.* Insofar as it is colorless, ethanol is an even more valuable probe molecule for tests under visible light because direct photolytic degradation is impossible. Figure 10 shows the DRIFT spectra recorded during photo-oxidation of ethanol vapor over melon−HT 150. Although the reaction is quite

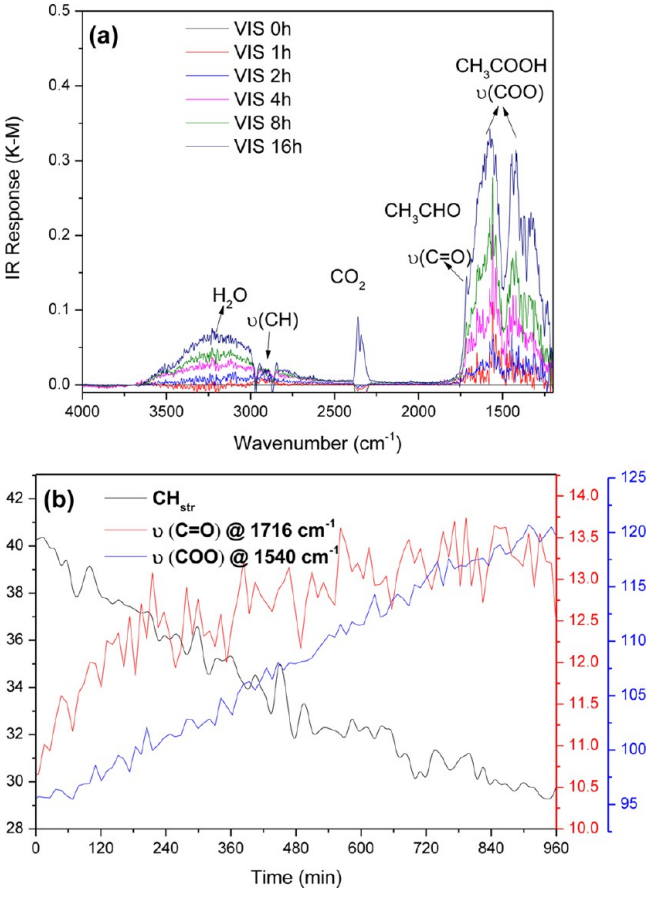


**Figure 10.** Photo-oxidation of ethanol vapor in air over melon−HT 150 under visible light irradiation.

slow, the spectroscopic behavior showed the progressive weakening of the ethanol bands and production of intermediates. Key intermediates, acetaldehyde and sorbed acetate species, were detected and grew over time at the expense of the C−H stretching band envelope of the ethyl moiety.

## DISCUSSION

**Formation of Melon on Different Samples.** The efficient formation of melon on a titanate surface rather than on anatase $TiO_2$ is evidently not due to textural effects per se because the loading on HT 200 (after calcination in $N_2$) was only slightly lower than that on HT 150 despite having only a fifth of the surface area of the latter (Table 2). Besides, when a

**Table 2. BET Surface Area Analysis of Mixed Samples Calcinated at 400 °C in Nitrogen Flow**

| | BET surface area ($m^2/g$) | |
|---|---|---|
| samples | before | after |
| urea−HT150 | 175.51 | 132.56 |
| urea−HT200 | 34.81 | 22.25 |
| urea−anatase | 8.82 | 12.02 |

control sample of Degussa P25 (~80% anatase, 20% rutile), with a surface area (50 $m^2/g$) exceeding that of HT 200, was used as substrate, the yield of melon was only around one-third of that formed on HT 200 (Table S2, Supporting Information).

Figure 11 compares DRIFT spectra of HT150, HT 200, and anatase $TiO_2$. At room temperature (RT), the broad absorption

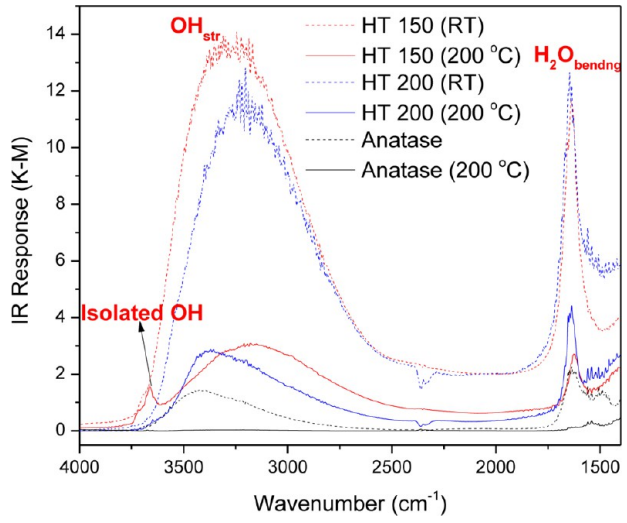


**Figure 11.** DRIFT spectra of HT 150, HT 200, and anatase $TiO_2$ at different temperatures.

band at 3300 $cm^{-1}$ is due to both surface OH stretching and adsorbed water. After heating at 200 °C to remove the latter, there are clearly more surface OH groups on HT 150 and HT 200 as compared to anatase $TiO_2$. Just as in a previous investigation,[30] isolated surface OH groups at ~3640, 3660 (strongest), and 3715 $cm^{-1}$ were evident, especially in HT 150. Hydrogen titanates as solid acid catalysts are known to bind compounds with a basic functionality strongly onto their surfaces.[28,34] This implies that titanates have a chemical functionality due to their rich surface OH groups and Brønsted


dx.doi.org/10.1021/sc400162p | ACS Sustainable Chem. Eng. 2014, 2, 149−157

acidic properties that promotes the conversion/polymerization of urea into melon because the formation of melon from urea is initiated by reaction with surface OH groups (eqs 1 −3).

**In Comparison with Graphitic Carbon Nitride.** Graphitic carbon nitride (g-$C_3N_4$) has the same tri-s-triazine units as melon but with a higher degree of polymerization; thus, a group of g-$C_3N_4$ modified samples were also studied to further clarify the mechanism. Compared with the pristine titania substrate, g-$C_3N_4$-modified samples show a small tail extending into the visible region (Figure 12a). The DRIFT spectrum of a g-$C_3N_4$-

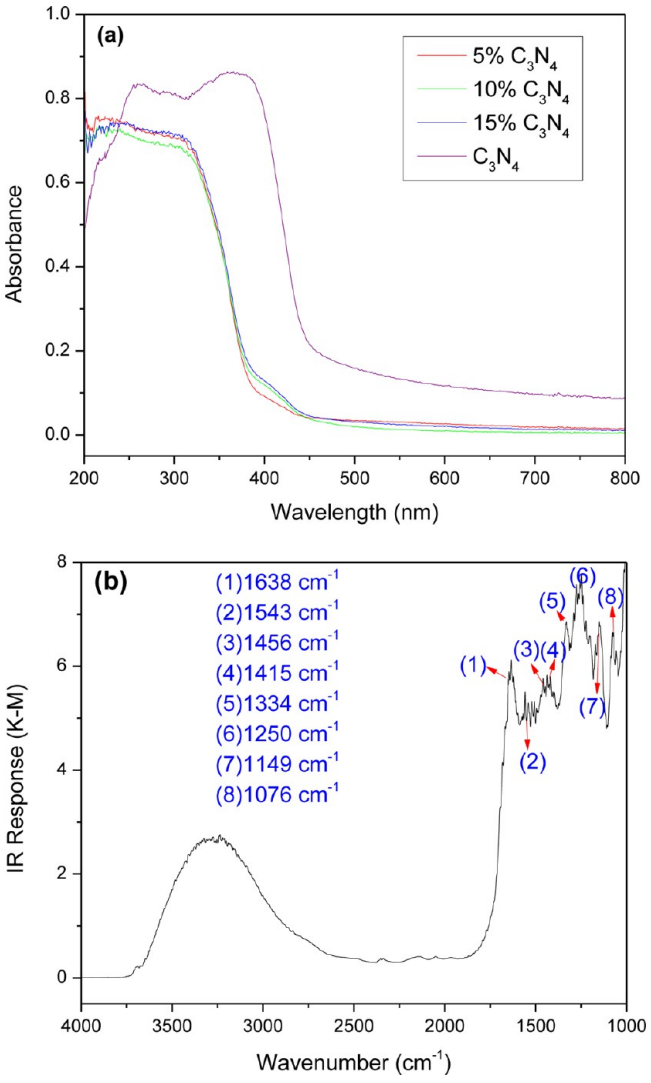


**Figure 12.** Characterization of g-$C_3N_4$ modified samples: (a) Diffuse reflectance UV−vis spectra and (b) DRIFT spectrum of 10 wt % g-$C_3N_4$-modified sample.

modified sample (Figure 12b) is very similar to the melon-modified one (Figure 7), indicating their structural similarity. However, the absence of distinct N−H bands at 3190 and 3300 $cm^{-1}$ in the former suggests the high degree of deamination of g-$C_3N_4$ in comparison with melon. Figure 13 shows their photocatalytic performance in MO degradation. Neither the pure $TiO_2$ substrate nor g-$C_3N_4$ itself showed significant photocatalytic activity, whereas all of the composites were active under visible irradiation (>385 nm). The promotion of photocatalytic activity of g-$C_3N_4$ by forming a hybrid structure with $TiO_2$ was also reported by Zhao et al.,[20] whereas Miranda

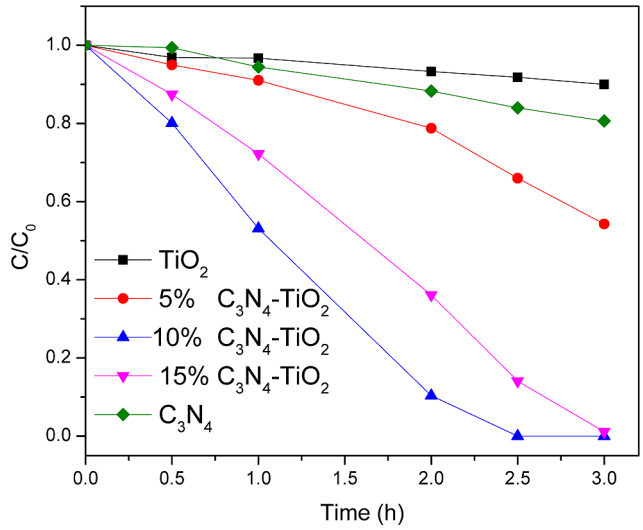


**Figure 13.** Photodegradation of MO by g-$C_3N_4$-modified samples under visible light (>385 nm) compared with unmodified anatase $TiO_2$ and g-$C_3N_4$ itself.

et al.[19] found no visible activity in phenol degradation even though a synergy was evident in the UV. In any event, this indicates that surface charge transfer between the two phases plays a key role in the photocatalytic activity.

Melon or g-$C_3N_4$ acts as a visible light sensitizer for titanate/$TiO_2$. As they are narrow gap semiconductors (2.8 eV),[16] visible light-induced interband transitions are excited just as in $TiO_2$. The relative band edge positions favor electron transfer (energetically downward) from melon or g-$C_3N_4$ to titanate/$TiO_2$ for oxygen activation (superoxide formation) with the more stable hole remaining on the nitride, hence the improvement in performance of the composite as compared to the separate phases. Protonation of formed superoxide radicals $O_2^{-}$• produces HOO • radicals, which could transform into $H_2O_2$ by further trapping electrons and finally into • OH radicals.[35,36] The hole left in the valence band of melon (g-$C_3N_4$) may be sufficient to displace protons from adsorbed $H_2O$ directly to produce •OH radicals that subsequently react with adsorbed organic species leading to their mineralization into $CO_2$ and $H_2O$. Presumably, there is an optimum loading of g-$C_3N_4$ or melon (10 wt % in this work), beyond which greater optical absorption in the visible by sensitizer layer build-up is eventually counterbalanced by inhibited access of $O_2$ to the underlying titanate/$TiO_2$.

Compared with melon-modified samples at the same loading, g-$C_3N_4$-modified samples show a better performance in MO degradation. This is possibly due to the better crystallinity (higher degree of polymerization) of g-$C_3N_4$, which reduces the probability of charge recombination.

## CONCLUSION

In this contribution, it was shown that titanates/$TiO_2$-bearing poly (tri-s-triazine) overlayers, viz., melon and g-$C_3N_4$ as photostable sensitizers, show far superior catalytic activity in both photodegradation of methyl orange (MO) dye and photo-oxidation of ethanol vapor under visible light irradiation, in comparison with the individual compounds. In addition, titanate substrates promote the spontaneous build-up of the melon overlayer due to the higher density coverage of titanates by surface OH groups and their Brønsted acidic properties and


dx.doi.org/10.1021/sc400162p | ACS Sustainable Chem. Eng. 2014, 2, 149−157

the related growth in photoactivity as compared to anatase $TiO_2$.

## ■ ASSOCIATED CONTENT

### Supporting Information

Elemental analysis results of mixed samples calcined at 400 °C in ambient air, elemental analysis result of mixture of urea and P25 $TiO_2$ calcined at 400 °C in $N_2$, and diffuse-reflectance UV−vis spectra of modified samples after calcination in air up to 800 °C. This material is available free of charge via the Internet at http://pubs.acs.org.

## ■ AUTHOR INFORMATION


### Corresponding Authors

*Tel.: +65 6796 3805. Fax: +65 6316 6182. E-mail: james_highfield@ices.a-star.edu.sg (J.G.H).

*Tel.: +65 6790 4256. Fax: +65 6790 9081. E-mail: aszchen@ntu.edu.sg (Z.C).


### Notes

The authors declare no competing financial interest.

## ■ ACKNOWLEDGMENTS

The authors thank the Environment and Water Industry Program Office (EWI) under the National Research Foundation of Singapore (Grant MEWR 651/06/160) for the financial support of this work. Valuable discussion with Dr. Ang Thiam Peng (ICES) is much appreciated. Technical assistances from Mr. Wong Hon Yue Kenneth (ICES) for surface area measurement and Ms. Chia Sze Chen (ICES) for NMR measurement are gratefully acknowledged.

## ■ REFERENCES


(1) Fujishima, A.; Honda, K. Electrochemical photolysis of water at a semiconductor electrode. *Nature* **1972**, *238* (5358), 37−38.

(2) Highfield, J. G.; Chen, M. H.; Nguyen, P. T.; Chen, Z. Mechanistic investigations of photo-driven processes over $TiO_2$ by in-situ DRIFTS-MS: Part 1. Platinization and methanol reforming. *Energy Environ. Sci.* **2009**, *2* (9), 991−1002.

(3) Fujishima, A.; Zhang, X. T.; Tryk, D. A. $TiO_2$ photocatalysis and related surface phenomena. *Surf. Sci. Rep.* **2008**, *63* (12), 515−582.

(4) Wang, R.; Hashimoto, K.; Fujishima, A.; Chikuni, M.; Kojima, E.; Kitamura, A.; Shimohigoshi, M.; Watanabe, T. Light-induced amphiphilic surfaces. *Nature* **1997**, *388* (6641), 431−432.

(5) Pichat, P. A brief overview of photocatalytic mechanisms and pathways in water. *Water Sci. Technol.* **2007**, *55* (12), 167−173.

(6) Chen, X.; Mao, S. S. Titanium dioxide nanomaterials: Synthesis, properties, modifications, and applications. *Chem. Rev.* **2007**, *107* (7), 2891−2959.

(7) Zhou, P.; Yu, J. G.; Wang, Y. X. The new understanding on photocatalytic mechanism of visible-light response N-S codoped anatase $TiO_2$ by first-principles. *Appl. Catal., B* **2013**, *142−143*, 45−53.

(8) Mitoraj, D.; Kisch, H. Surface modified titania visible light photocatalyst powders. *Solid State Phenom.* **2010**, *162*, 49−75.

(9) Mitoraj, D.; Kisch, H. On the mechanism of urea-induced titania modification. *Chem.—Eur. J.* **2010**, *16* (1), 261−269.

(10) Mitoraj, D.; Kisch, H. The nature of nitrogen-modified titanium dioxide photocatalysts active in visible light. *Angew. Chem., Int. Ed.* **2008**, *47* (51), 9975−9978.

(11) Kisch, H. Semiconductor photocatalysis mechanistic and synthetic aspects. *Angew. Chem., Int. Ed.* **2013**, *52* (3), 812−847.

(12) Ang, T. P.; Chan, Y. M. Comparison of the melon nanocomposites in structural properties and photocatalytic activities. *J. Phys. Chem. C* **2011**, *115* (32), 15965−15972.

(13) Liebig, J. Ueber einige stickstoffverbindungen. *Ann. Phys.* **1835**, *110* (4), 570−613.

(14) Schwarzer, A.; Saplinova, T.; Kroke, E. Tri-s-triazines (s-heptazines)—From a "mystery molecule" to industrially relevant carbon nitride materials. *Coord. Chem. Rev.* **2013**, *257* (13−14), 2032−2062.

(15) Wang, X.; Blechert, S.; Antonietti, M. Polymeric graphitic carbon nitride for heterogeneous photocatalysis. *ACS Catal.* **2012**, *2* (8), 1596−1606.

(16) Wang, Y.; Wang, X. C.; Antonietti, M. Polymeric graphitic carbon nitride as a heterogeneous organocatalyst: From photochemistry to multipurpose catalysis to sustainable chemistry. *Angew. Chem., Int. Ed.* **2012**, *51* (1), 68−89.

(17) Zhang, J. S.; Chen, X. F.; Takanabe, K.; Maeda, K.; Domen, K.; Epping, J. D.; Fu, X. Z.; Antonietti, M.; Wang, X. C. Synthesis of a carbon nitride structure for visible-light catalysis by copolymerization. *Angew. Chem., Int. Ed.* **2010**, *49* (2), 441−444.

(18) Wang, X. C.; Maeda, K.; Thomas, A.; Takanabe, K.; Xin, G.; Carlsson, J. M.; Domen, K.; Antonietti, M. A metal-free polymeric photocatalyst for hydrogen production from water under visible light. *Nat. Mater.* **2009**, *8* (1), 76−80.

(19) Miranda, C.; Mansilla, H.; Yanez, J.; Obregon, S.; Colon, G. Improved photocatalytic activity of g-$C_3N_4$/$TiO_2$ composites prepared by a simple impregnation method. *J. Photochem. Photobio., A* **2013**, *253*, 16−21.

(20) Zhao, S. S.; Chen, S.; Yu, H. T.; Quan, X. g-$C_3N_4$/$TiO_2$ hybrid photocatalyst with wide absorption wavelength range and effective photogenerated charge separation. *Sep. Purif. Technol.* **2012**, *99*, 50−54.

(21) Sun, X. M.; Li, Y. D. Synthesis and characterization of ion-exchangeable titanate nanotubes. *Chem.—Eur. J.* **2003**, *9* (10), 2229−2238.

(22) Bavykin, D. V.; Friedrich, J. M.; Walsh, F. C. Protonated titanates and $TiO_2$ nanostructured materials: Synthesis, properties, and applications. *Adv. Mater.* **2006**, *18* (21), 2807−2824.

(23) Gong, D. G.; Ho, W. C. J.; Tang, Y. X.; Tay, Q.; Lai, Y. K.; Highfield, J. G.; Chen, Z. Silver decorated titanate/titania nanostructures for efficient solar driven photocatalysis. *J. Solid State Chem.* **2012**, *189*, 117−122.

(24) Bavykin, D. V.; Walsh, F. C. Elongated titanate nanostructures and their applications. *Eur. J. Inorg. Chem.* **2009**, *8*, 977−997.

(25) Yang, D. J.; Liu, H. W.; Zheng, Z. F.; Yuan, Y.; Zhao, J. C.; Waclawik, E. R.; Ke, X. B.; Zhu, H. Y. An efficient photocatalyst structure: $TiO_2$(B) nanofibers with a shell of anatase nanocrystals. *J. Am. Chem. Soc.* **2009**, *131* (49), 17885−17893.

(26) Zhu, H. Y.; Gao, X. P.; Lan, Y.; Song, D. Y.; Xi, Y. X.; Zhao, J. C. Hydrogen titanate nanofibers covered with anatase nanocrystals: A delicate structure achieved by the wet chemistry reaction of the titanate nanofibers. *J. Am. Chem. Soc.* **2004**, *126* (27), 8380−8381.

(27) Yang, H. G.; Zeng, H. C. Synthetic architectures of $TiO_2$/$H_2Ti_5O{\cdot}H_2O$, ZnO/$H_2Ti_5O{\cdot}H_2O$, ZnO/$TiO_2$/$H_2Ti_5O_{11}{\cdot}H_2O$, and ZnO/$TiO_2$ nanocomposites. *J. Am. Chem. Soc.* **2005**, *127* (1), 270−278.

(28) Kitano, M.; Nakajima, K.; Kondo, J. N.; Hayashi, S.; Hara, M. Protonated titanate nanotubes as solid acid catalyst. *J. Am. Chem. Soc.* **2010**, *132* (19), 6622−6623.

(29) Cheng, Y. H.; Huang, Y. Z.; Kanhere, P. D.; Subramaniam, V. P.; Gong, D. G.; Zhang, S.; Highfield, J.; Schreyer, M. K.; Chen, Z. Dual-phase titanate/anatase with nitrogen doping for enhanced degradation of organic dye under visible light. *Chem.—Eur. J.* **2011**, *17* (9), 2575−2578.

(30) Cheng, Y. H.; Subramaniam, V. P.; Gong, D. G.; Tang, Y. X.; Highfield, J.; Pehkonen, S. O.; Pichat, P.; Schreyer, M. K.; Chen, Z. Nitrogen-sensitized dual phase titanate/titania for visible-light driven phenol degradation. *J. Solid State Chem.* **2012**, *196*, 518−527.

(31) Ang, T. P. Sol-gel synthesis of a novel melon-$SiO_2$ nanocomposite with photocatalytic activity. *Catal. Commun.* **2009**, *10* (14), 1920−1924.

(32) Jurgens, B.; Irran, E.; Senker, J.; Kroll, P.; Muller, H.; Schnick, W. Melem (2,5,8-triamino-tri-s-triazine), an important intermediate during condensation of melamine rings to graphitic carbon nitride:

Synthesis, structure determination by X-ray powder diffractometry, solid-state NMR, and theoretical studies. *J. Am. Chem. Soc.* **2003**, *125* (34), 10288−10300.
(33) Lotsch, B. V.; Döblinger, M.; Sehnert, J.; Seyfarth, L.; Senker, J.; Oeckler, O.; Schnick, W. Unmasking melon by a complementary approach employing electron diffraction, solid-state NMR spectroscopy, and theoretical calculations—Structural characterization of a carbon nitride polymer. *Chem.—Eur. J.* **2007**, *13* (17), 4969−4980.
(34) Goncalves, R. H.; Schreiner, W. H.; Leite, E. R. Synthesis of $TiO_2$ nanocrystals with a high affinity for amine organic compounds. *Langmuir* **2010**, *26* (14), 11657−11662.
(35) Yu, J. G.; Dai, G. P.; Xiang, Q. J.; Jaroniec, M. Fabrication and enhanced visible-light photocatalytic activity of carbon self-doped $TiO_2$ sheets with exposed {001} facets. *J. Mater. Chem.* **2011**, *21* (4), 1049−1057.
(36) Xiang, Q. J.; Yu, J. G.; Wong, P. K. Quantitative characterization of hydroxyl radicals produced by various photocatalysts. *J. Colloid Interface Sci.* **2011**, *357* (1), 163−167.